PHYSICAL REVIEW B VOLUME 22, NUMBER 4 15 AUGUST 1980

Intra- and inter-valence-band electronic Raman scattering in heavily doped p-GaAs

Diego Olego and Manuel Cardona
Max-Planck-Institut für Festkörperforschung, Heisenbergstrasse 1, 7000 Stuttgart 80, Federal Republic of Germany

Ulrich Rössler
Universität Regensburg, Fakultät für Physik, Universitätsstrasse 31, 8400 Regensburg, Federal Republic of Germany
(Received 8 February 1980)

Two features have been observed in the emission spectra of heavily Zn-doped GaAs, with Stokes shifts in the energy range between 10 and 400 meV. They are attributed to intra- and inter-valence-band electronic Raman scattering involving the heavy- and light-hole valence bands. The measured Stokes shifts of these features depend on the incident photon energy and on the free-hole concentrations of the samples. Both dependences can be explained by means of the following resonant Raman process: from the valence bands to intermediate states in the conduction band and back to empty valence states near the Fermi level. These processes also account semiquantitatively for the dependence of the observed structure on the polarization of incident and scattered light.

INTRODUCTION

The inelastic scattering of light by electronic excitations in semiconductors (electronic Raman scattering) has been extensively investigated in recent years.[1] The electronic Raman scattering (ERS) can be viewed as a second-order process in which two photons are involved. By absorbing an incident photon an electron undergoes a transition from its initial energy state to an intermediate one; a second photon is emitted as the photoexcited electron makes a transition to its final energy state. The measured Raman shift (usually Stokes) corresponds to the energy difference between the final and initial electronic energy states. When both states belong to the same energy band, the scattering is referred to as intra-band ERS. If they are in different energy bands the scattering is called inter-band. Both types of ERS have been theoretically and experimentally studied in heavily doped semiconductors.[1-5] A typical material for this kind of investigation is p-type Si. When the Fermi level lies below the top of the valence bands, intra-valence-band as well as inter-valence-band ERS from filled to empty valence states is possible.[4] The presence of the inter-valence-band ERS has been strikingly evidenced in p-Si because of its interference with the zone-center optical phonon.[6] These inter-band transitions are infrared forbidden by parity at the center of the Brillouin zone (they can nevertheless be observed[7]). Correspondingly they are Raman allowed and form a continuum which overlaps with the frequency of the optical phonon. Some indication of the existence of ERS involving the valence bands has also been inferred from the line shape of the phonon Raman spectra of heavily doped p-Ge and p-GaAs.[8]

In this paper we report the observation of intra-valence-band as well as inter-valence-band ERS in heavily doped p-GaAs. The measured Stokes energy shifts for both types of processes depend slightly on the frequency of the incident photons. This behavior, unusual in the case of nonresonant Raman scattering, is explained by invoking resonant processes involving *real* (as opposed to virtual) electronic transitions as the incident photons are absorbed. As in most such processes involving *real* intermediate states, the contribution, at least in part, of hot luminescence[9,10] cannot be completely excluded.

The Stokes shifts reported here also depend on the free-hole concentrations of the samples (i.e., on the Fermi energies). This dependence is explained by assuming that the electrons photoexcited to the conduction band (intermediate states) make non-$\vec{k}$-conserving (indirect) transitions to empty valence states near the Fermi level (final states). With some additional assumptions, the model is also able to explain the strong polarization effects observed. The observed processes thus represent, to the extent in which they can be described by our model as ERS, the instantaneous response to the optical excitation process (no relaxation of the electron in the intermediate states). This work complements the luminescence studies at the direct gap E_0, where the effect of direct and indirect transitions on the recombination processes has also been recognized.[11]

I. EXPERIMENT

The samples were cut from Zn-doped GaAs single crystals and their free-hole concentrations

 © 1980 The American Physical Society

determined by means of Hall measurements. Surfaces with a [110] orientation, either cleaved or polished and etched with an aqueous solution of NaOCl, were used. The samples were glued with silver paste to a copper cold finger, which was placed in an evacuated glass Dewar and maintained in contact with a liquid-nitrogen bath.

The measurements were performed in the standard backscattering geometry. Different lines of an Ar^+-ion laser were used for excitation. The scattered light was analyzed with a Spex 0.8-m double monochromator and detected with an RCA 31034 photomultiplier equipped with photon-counting electronics. The counts were stored on a multichannel analyzer with typical integration times per channel ranging from 5 to 10 s and a spacing of ~5 cm^{-1} between adjacent channels. The shapes of the recorded spectra were independent of the surface preparation (cleaved or polished etched).

II. RESULTS

Figure 1 displays typical Stokes spectra of GaAs with 9×10^{19} holes cm^{-3} recorded at 80 K between 10 and 400 meV. The spectra were excited with different incident photon energies. Besides the Raman-active transverse optical phonon (TO), two broad structures (labeled A and B) are observed on the Stokes side of the emission. Both structures shift to different energies as the incident photon energy is changed; their Stokes shifts become *larger* with *increasing* incident photon energy. This behavior is also observed in the Stokes spectra of the samples with 4×10^{19} and 1.6×10^{19} holes cm^{-3}. For Stokes shifts larger than 400 meV the emission spectra reproduce the luminescence features reported previously.[12]

Typical spectra for a given incident photon energy and different free-hole concentrations at 80 K are displayed in Fig. 2. When the hole concentration is *decreased, larger* Stokes shifts of the structures A and B are observed. The energy difference between the Stokes shifts of either peak A or B for two different hole concentrations is approximately equal to the difference between the corresponding Fermi energies. We have measured for the Fermi energies 116, 84, and 45 meV, for the samples with 9×10^{19}, 4×10^{19}, and 1.6×10^{19} holes cm^{-3}, respectively.[11] This behavior is the same for other incident photon energies. The dependence of the Stokes shifts of the structures

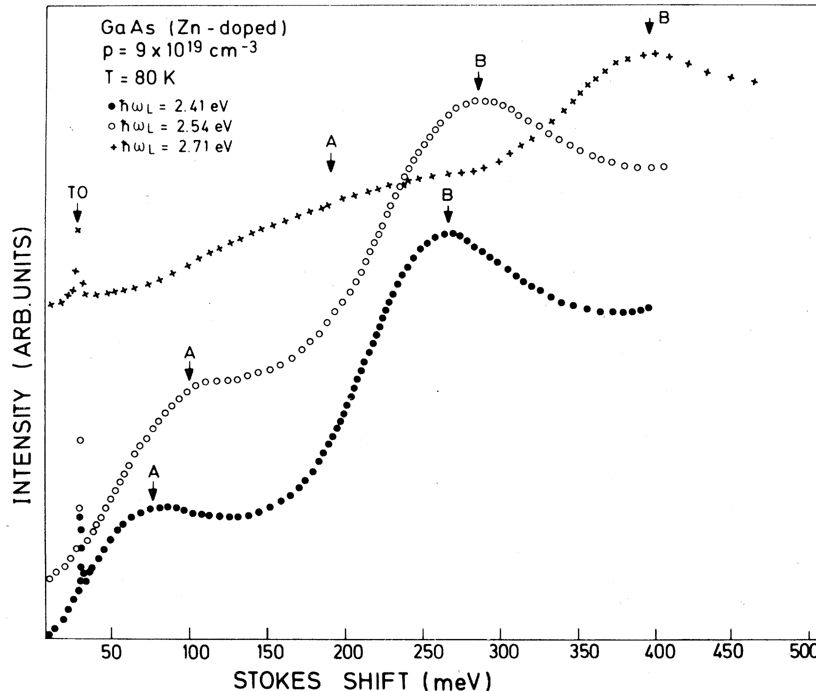

FIG. 1. Stokes spectra of p-GaAs with 9×10^{19} holes cm^{-3} obtained at 80 K with three different incident-photon energies. The spectra show beside the optical phonon Raman line (TO) two structures (A and B) which shift slightly to higher energies with increasing incident-photon energy. The structure A is interpreted in the text as intra-valence-band electronic Raman scattering and the structure B as its inter-valence-band counterpart. The measurements were performed on a {110} face and the incident and scattered fields were parallel to the $[1\bar{1}0]$ direction. For this scattering configuration the $\Gamma_1+\Gamma_{12}+\Gamma_{15}$ combination of irreducible representations is measured.

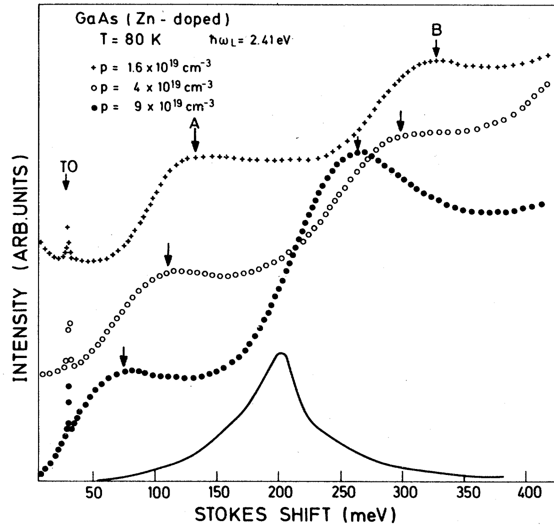

FIG. 2. Stokes spectra of p-GaAs with different hole concentrations at 80 K. The incident-photon energy was fixed at 2.41 eV. With decreasing hole concentration the structures A and B shift to higher energies. The spectra were obtained with the scattering configuration described in in the caption of Fig. 1. The solid line represents the inter-valence-band Raman scattering cross section for the sample with 4×10^{19} holes cm^{-3} calculated for $\hbar\omega_L = 2.41$ eV assuming $\vec{k}$ conservation in the matrix elements of Eq. (1).

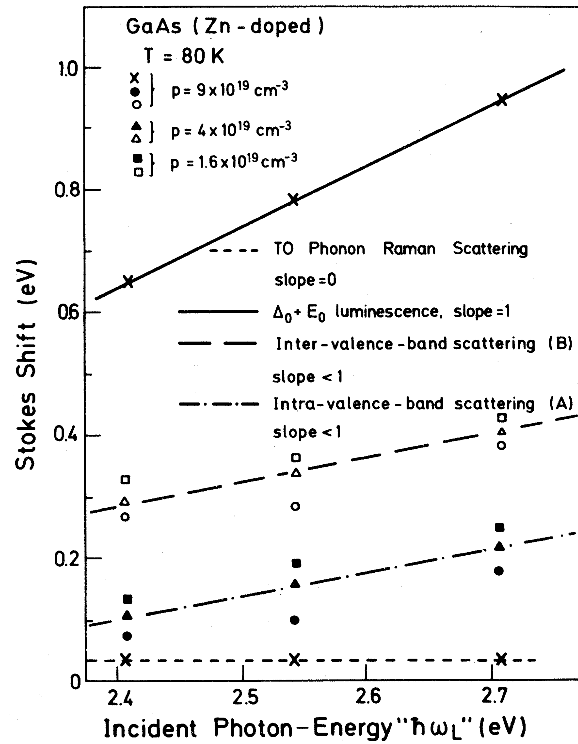

FIG. 3. Dependence on the incident-photon energy of the $E_0+\Delta_0$ luminescence peak (Ref. 12), the intra- and inter-valence-band scattering structures, and the phonon Raman scattering.

A and B on the incident photon energy and on the free-hole concentration is given by the triangles, squares, and circles of Fig. 3 (see also Table I).

III. DISCUSSION

In order to elucidate the nature of peaks A and B we have plotted in Fig. 3 their Stokes shifts as a function of laser frequency ω_L. We have also plotted in this figure the corresponding Stokes shifts of a typical *cold* luminescence process, the $E_0+\Delta_0$ emission of GaAs[12] and that of a typical Raman process (e.g., the TO phonons of Fig. 1, independent of ω_L). The Stokes shifts of peaks A and B occupy an intermediate position, somewhat closer, however, to the Raman than to the luminescence case. Since the laser photons used in our experiment have an energy within the continuum of direct valence to conduction-band transitions in GaAs we must be dealing with a possible continuum of real intermediate states. Under these conditions the observed features may be due to either ERS, hot luminescence, or, most likely, a mixture thereof. We consider ERS to involve well-defined intermediate states $|c\rangle$ with the resonant scattering amplitude given by[1,2]

$$R_{\mu\nu}=\frac{1}{m}\sum_{c\vec{k}}\frac{\langle v_f|p_\mu|c\rangle\langle c|p_\nu|v_i\rangle}{\hbar\omega_L-[E_c(\vec{k})-E_i(\vec{k})]+i\Gamma}\,. \tag{1}$$

In our case $|c\rangle$ represents conduction-band states, $|v_i\rangle$ filled valence (initial) states, and $|v_f\rangle$ empty (final) valence states. Γ represents the width of the energy states. We shall show in what follows that there are Raman processes within the known energy-band scheme of GaAs which explain most of the properties of peaks A and B. A contribution of luminescence, in particular of elastic processes producing the loss of phase coherence in the intermediate state, cannot be completely excluded.

Due to the continuum of the combined density of states there is some $\vec{k}\neq0$ for which the energy difference $E_c(\vec{k})$-$E_v(\vec{k})$ matches the energy of the lines of an Ar^+-ion laser, represented by $\hbar\omega_L$ in Eq. (1): A strong resonance of the scattering represented by Eq. (1) is expected in these cases. Hence the Raman shift may depend on the incident-photon energy: the resonant-energy denominator enhances transitions involving particular initial and final states. These transitions determine the observed Stokes shift, thus accounting for the difference in slopes between the ERS process and the phonon Raman scattering as displayed in Fig. 3. It is customary to assume

TABLE I. Stokes shifts of the peak maxima A and B as a function of incident-photon energy and of free-hole concentrations. The experimental error of the measured values is ±10 meV. The calculated Stokes shifts were obtained as displayed in Fig. 4.

		A-Stokes shifts (meV)			B-Stokes shifts (meV)		
p (cm^{-3})		$\hbar\omega_L$=2.41 eV	$\hbar\omega_L$=2.54 eV	$\hbar\omega_L$=2.71 eV	$\hbar\omega_L$=2.41 eV	$\hbar\omega_L$=2.54 eV	$\hbar\omega_L$=2.71 eV
9×10^{19}	measured	75	100	188	270	282	390
	calculated	102 [a]		180 [a]	244 [a]		330 [a]
		0 [b]		0 [b]	230 [b]		290 [b]
		0 [c]		0 [c]	150 [c]		190 [c]
4×10^{19}	measured	110	167	225	295	345	410
	calculated	132 [a]		220 [a]	270 [a]		350 [a]
		0 [b]		10 [b]	260 [b]		320 [b]
		12 [c]		54 [c]	180 [c]		220 [c]
1.6×10^{19}	measured	131	195	248	330	366	440
	calculated	170 [a]		252 [a]	310 [a]		392 [a]
		40 [b]		54 [b]	290 [b]		360 [b]
		50 [c]		94 [c]	220 [c]		264 [c]

[a] For $\vec{k}$ along [100].
[b] For $\vec{k}$ along [110].
[c] For $\vec{k}$ along [111].

$\vec{k}$ conservation in the evaluation of the matrix elements of expressions of the type of Eq. (1). We have evaluated Eq. (1) by performing the $\vec{k}$ sum with the energy of the valence bands obtained by diagonalization of the 6×6 Luttinger matrix for each $\vec{k}$ with the parameters of Ref. 13 and the conduction bands including nonparabolicity[14,15] and gap shrinkage due to impurities and free carriers.[11] The result for $p=4\times10^{19}$ holes cm^{-3} is shown by the solid curve of Fig. 2. The peak obtained does not correspond to the experimental data, although it may be argued that the experimental data can be obtained by symmetrically splitting the calculated solid line.

In view of the impossibility of explaining our results on the basis of direct transitions we try to use in Eq. (1) one direct matrix element (from $|v_i\rangle$ to $|c\rangle$) and an indirect one (from $|c\rangle$ to $|v_f\rangle$). The latter process is to be viewed as induced by the impurity potential which breaks down the translational symmetry. One may treat this breakdown by considering the intermediate state $|c\rangle$ of Eq. (1) to be a scattering state of the band electrons in the random potential of the impurities. Equivalently the corresponding matrix element could be decomposed into a non-$\vec{k}$-conserving transition to an intermediate state most likely in the lowest conduction band, followed by a $\vec{k}$-conserving transition with p_μ. Similar indirect processes play an important role in luminescence[11] and in scattering by indirect coupled phonon-plasmon modes.[16]

Figure 4 shows schematically the type of process we have in mind. The band structure in this figure has been obtained as mentioned above for $\vec{k}$ along [100] (we have performed similar calculations for the [110] and [111] directions). The direct process, involving the laser photon, is chosen to be resonant (real intermediate state) and to initiate in either the light (process B) or the heavy-hole band (process A). The slightly indirect process ends at the Fermi level of the heavy-hole band, where the density of empty states is maximum. The energy difference $(E_F - E_i)$ between the Fermi energy (E_F) and the energy of the initial state (E_i) yields the corresponding Stokes shifts. We show in Table I the Stokes shifts of the A and B peaks calculated for the [100], [110], and [111] directions as indicated in Fig. 4 with $\hbar\omega_L$ equal to 2.41 and 2.71 eV. For peak B both [100] and [110] transitions are able to explain the experimental results (also shown in Table I) within the uncertainty of the data. The onset of the scattering corresponds to the [111] transitions. The near degeneracy of [110] and [100] shifts guarantees a large density of states for the processes, as required for the interpretation of the experimental peak. The experimental peak A corresponds solely to the calculated transitions along [100]. The model proposed in Fig. 4 and Table I explains both (a) the dependence of the Stokes shifts on the incident-photon energy because for each exciting energy different initial states E_i are involved, and (b) the Stokes shifts to higher energies with decreasing free-hole concentrations because for a given E_i (determined

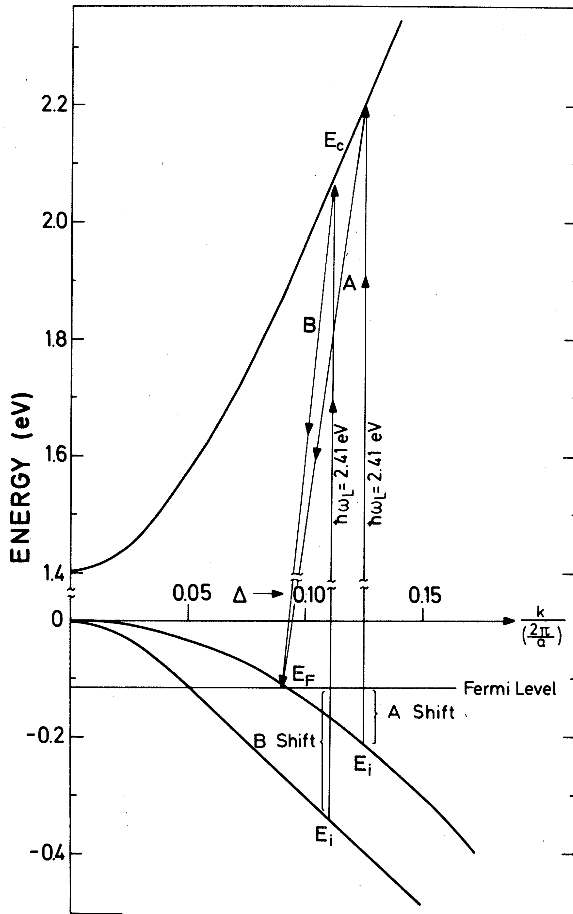

FIG. 4. Conduction and valence bands of GaAs near the Γ point for $\vec{k} \parallel [100]$. The arrows represent the ERS under discussion and show how the A and B Stokes shifts are determined. The initial state with energy E_i is fixed by the condition $E_c - E_i = \hbar\omega_L$. The energy difference $E_F - E_i$ represents the corresponding Stokes shift.

by the incident-photon energy) the differences $E_F - E_i$ ($\simeq$Stokes shifts) become larger as the free-hole concentration decreases. The model accounts also for the observation that for a given incident energy the differences between the Stokes shifts for two-hole concentrations are approximately the difference between the corresponding Fermi energies.

The scattering at energies around the TO phonon (33 meV)[8] arises from A transitions with initial states along the [111] and [110] directions. For concentrations of 4×10^{19} and 9×10^{19} holes cm^{-3} the initial states along these directions are degenerate with the Fermi energy, a fact which allows scattering with very small Stokes shifts ($E_F - E_i \simeq 0$). For the sample with 1.6×10^{19} holes cm^{-3} there is an onset for the scattering at low energies because the difference $E_F - E_i$ is finite even for initial states along the [110] and [111] directions. In Fig. 2 the spectrum of the sample with 1.6×10^{19} holes cm^{-3} shows that the intra-valence-band ERS begins at energies larger than 50 meV, and no interference between the TO phonon energy and the ERS takes place. For the TO phonons of this sample no self-energy effects were measured.[8,16]

In Ref. 11 we studied the photoluminescence at the direct E_0 energy gap of heavily doped p-GaAs and showed that at low temperatures the high-energy side of the recombination spectra is dominated by indirect transitions from the bottom of the conduction band to the Fermi level of the valence bands. The processes discussed here are similar except for the lack of relaxation within the conduction band. Consequently we consider the measured scattering within our model as the response to the optical-excitation process in which the photoexcited electrons recombine without previous relaxation in the conduction band, as illustrated in Fig. 4. This point of view implies that no loss of coherence (i.e., phase randomization) occurs while the electrons are in the intermediate state $|c\rangle$. If some loss of coherence occurs the processes would involve some *hot luminescence*.

The preservation of coherence can be best tested by investigating the polarization-selection rules. A complete investigation would involve a study for incident linear and circular polarization of the amount of unpolarized, linearly polarized, and circularly polarized (with sign) scattered light. In view of the weak and broad signals obtained for the features under consideration we have not, at present, performed such a complete study (it will be the object of future work). We have, instead, performed three independent measurements with *linearly* polarized light, as shown in Fig. 5 for a sample with 9×10^{19} holes cm^{-3} at 80 K. Under the assumption of no *unpolarized* scattered components, the measurements of Fig. 5 allow for the determination of the Γ_1, Γ_{12}, and $\Gamma_{15}+\Gamma_{25}$ components of the Raman tensors. Even then, an accurate determination of the amounts by which these irreducible representations contribute to the observed features A and B is difficult because of the large background present, due probably to luminescence.[11,12] We can, however, establish that scattering of Γ_1 symmetry is stronger in the intra-valence-band feature A. For this configuration some contribution of scattering with $\Gamma_{15}+\Gamma_{25}$ symmetry is also detectable. The $\Gamma_{15}+\Gamma_{25}$ terms dominate the inter-valence-band ERS processes (B), where the Γ_{12} and Γ_1 symmetries are also present. The ratio of these components measured for two different incident-

TABLE II. Ratios of the irreducible representations present in the intra- and inter-valence-band scattering for p-GaAs with 9×10^{19} holes cm^{-3} at $T=80$ K. The measured ratios are affected by an uncertainty of ±50%. The estimated ones were calculated by evaluation of the Raman tensor of Eq. (1) with the valence-band wave functions near $\vec{k}=0$.

$\hbar\omega_L$ (eV)	Intra-valence-band scattering (A)		Inter-valence-band scattering (B)	
2.41	$\frac{\Gamma_1}{\Gamma_{15}+\Gamma_{25}}=2.4$	$\frac{\Gamma_1}{\Gamma_{12}}=15$	$\frac{\Gamma_{15}+\Gamma_{25}}{\Gamma_1}=4.3$	$\frac{\Gamma_{15}+\Gamma_{25}}{\Gamma_{12}}=4.3$
2.51	$\frac{\Gamma_1}{\Gamma_{15}+\Gamma_{25}}=1.8$	$\frac{\Gamma_1}{\Gamma_{12}}=6$	$\frac{\Gamma_{15}}{\Gamma_1}=3.2$	$\frac{\Gamma_{15}}{\Gamma_{12}}=4.6$
Calculated $\vec{k}\parallel[100]$	$\frac{\Gamma_1}{\Gamma_{15}+\Gamma_{25}}=1.3$	$\frac{\Gamma_1}{\Gamma_{12}}=8$	$\frac{\Gamma_{15}+\Gamma_{25}}{\Gamma_1}=\infty$	$\frac{\Gamma_{15}+\Gamma_{25}}{\Gamma_{12}}=10$
$\vec{k}\parallel[110]$	$\frac{\Gamma_1}{\Gamma_{15}+\Gamma_{25}}=1.1$	$\frac{\Gamma_1}{\Gamma_{12}}=32$	$\frac{\Gamma_{15}+\Gamma_{25}}{\Gamma_1}=\infty$	$\frac{\Gamma_{15}+\Gamma_{25}}{\Gamma_{12}}=5$
$\vec{k}\parallel[100]$ and $\vec{k}\parallel[110]$	$\frac{\Gamma_1}{\Gamma_{15}+\Gamma_{25}}=1.15$	$\frac{\Gamma_1}{\Gamma_{12}}=16$	$\frac{\Gamma_{15}+\Gamma_{25}}{\Gamma_1}=\infty$	$\frac{\Gamma_{15}+\Gamma_{25}}{\Gamma_{12}}=6$

photon energies are listed in Table II. The $\Gamma_{15}+\Gamma_{25}$ component of the A features provides the continuum which overlaps with transverse optical phonon, also of symmetry Γ_{15}.[8] By replacing for $|v_i\rangle$ and $|v_f\rangle$ in Eq. (1) the well-known valence-band wave functions near $\vec{k}=0$, the Raman tensors for the intra- and intervalence-band scattering processes can be evaluated for different directions of $\vec{k}$. These estimates should be accurate if $E_F \ll$ the spin-orbit splitting Δ_0 (which holds in our case) and if the impurity potential can be considered to have Γ_1 symmetry (probably a good approximation for very heavily doped samples). They show that the main contributions to the intra-valence-band ERS have Γ_1 symmetry, while for the inter-valence-band ERS the $\Gamma_{15}+\Gamma_{25}$ component dominates (see Table II). This agrees semi-quantitatively with our experimental results, except for the unexpected (although weak) Γ_1 component of the B feature. This Γ_1 component may be due either to components of the impurity potential other than Γ_1 or to hot luminescence. The degree of polarization of the B line should be carefully investigated.

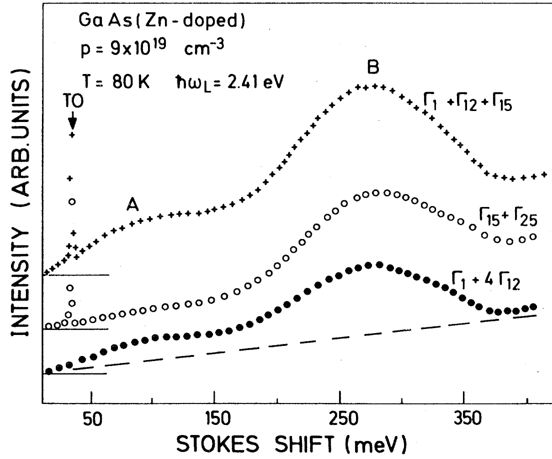

FIG. 5. Polarization dependence of the intra- and inter-valence-band scattering for p-GaAs with 9×10^{19} holes cm^{-3} at 80 K. The measurements were performed on a {110} face with an incident-photon energy of 2.41 eV. The $\Gamma_1+\Gamma_{12}+\Gamma_{15}$ combination of irreducible representations was obtained with the incident and scattered fields parallel to the $[1\bar{1}0]$ direction, the $\Gamma_1+4\Gamma_{12}$ combination with the incident and scattered fields parallel to [001], and the $\Gamma_{15}+\Gamma_{25}$ representation with the incident field parallel to $[1\bar{1}0]$ and the scattered one parallel to [001]. The horizontal lines represent the estimated zero of scattering intensity. The dashed line represents the typical background assumed for the evaluation of the ratios of the different irreducible representations listed in Table II.

CONCLUSIONS

Intra- and inter-valence-band electronic Raman scattering has been reported for heavily Zn-doped GaAs. The intra-valence-band scattering involves initial and final states in the heavy-hole valence bands. The dominant symmetry of this process is Γ_1 with some contribution of $\Gamma_{15}+\Gamma_{25}$. The Stokes shifts of the peak maxima seem to be mainly determined by initial states along the [100] directions. The inter-valence-band scattering corresponds to transitions from initial states in the light-hole valence bands to final states in the heavy-hole valence bands. $\Gamma_{15}+\Gamma_{25}$ symmetry is dominant for this scattering process. Initial states along the [110] and [100] directions determine the Stokes shifts of the peak maxima.

ACKNOWLEDGMENTS

One of us (D.O.) wants to acknowledge helpful discussions with Dr. M. Chandrasekhar, Dr. M. Grimsditch, and Dr. R. Merlin during the early stages of this work and the Deutscher Akademischer Austauschdienst for the granting of a fellowship. The technical assistance of H. Hirt and the help of E. Kisela in sample preparation are gratefully acknowledged.

[1]For a review see, for example, M. V. Klein, in *Light Scattering in Solids*, edited by M. Cardona (Springer Berlin, 1975), p. 205 and references therein.

[2]D. L. Mills, R. F. Wallis, and E. Burstein, in *Light Scattering in Solids*, edited by M. Balkanski (Flammarion, Paris, 1971), p. 107.

[3]M. Chandrasekhar, M. Cardona, and E. O. Kane, Phys. Rev. B 16, 3579 (1977).

[4]M. Chandrasekhar, U. Rössler, and M. Cardona, in *Physics of Semiconductors 1978*, edited by B. Wilson (The Institute of Physics, London, 1978), p. 961.

[5]J. Geurts and W. Richter, Ref. 4, p. 513.

[6]F. Cerdeira, T. A. Fjeldly, and M. Cardona, Phys. Rev. B 8, 4734 (1973).

[7]R. Braunstein and E. O. Kane, J. Phys. Chem. Solids 23, 1423 (1962).

[8]D. Olego, H. R. Chandrasekhar, and M. Cardona, Ref. 4, p. 1313.

[9]M. Cardona, Ref. 1, p. 1 and other references therein.

[10]B. P. Zakharchenya, V. I. Zemskii, and D. N. Mirlin, Fiz. Tverd. Tela (Leningrad) 19, 1725 (1977) [Sov. Phys.—Solid State 19, 1006 (1977)].

[11]D. Olego and M. Cardona, Phys. Rev. B 22, 869 (1980).

[12]D. Olego and M. Cardona, Solid State Commun. 32, 1027 (1979).

[13]U. Rössler, in *Festkörperprobleme XIX* (Adv. in Solid State Phys.) edited by J. Treusch (Vieweg, Weisbaden, 1979), p. 77.

[14]M. Cardona, Phys. Rev. 121, 752 (1961).

[15]M. Cardona, in *Atomic Structure and Properties of Solids*, edited by E. Burstein (Academic, New York, 1972), p. 514.

[16]D. Olego and M. Cardona, Solid State Commun. 32, 375 (1979).